

MR Imaging of Asherman's Syndrome in Patients With and Without Uterine Anomalies : Comparison with Hysterosalpingography¹

Jung Sik Kim, M.D., Hong Kim, M.D., Taek Hoon Kim, M.D.²

Purpose : To assess the role of MR imaging in the detection of Asherman's syndrome, especially when this is associated with a congenital uterine anomaly.

Materials and Methods : MR images were obtained in the semicoronal plane parallel to the long axis of the uterus in 11 patients. Dilatation and curettage involving the insertion of an intrauterine device was performed in all patients, and transabdominal metroplasty was performed in four with uterine anomaly. MR imaging findings were compared with those of hysterosalpingography in all patients and compared with surgical findings in four.

Results : The MR findings of uterine synechia demonstrated in nine of 11 patients were focal thickening of the uterine junctional zone (n=2), hypointense foci in the endometrium (n=1), or both these findings (n=6). Seven of the 11 patients had associated uterine anomalies, which were demonstrated in all seven by MR imaging. In four of the seven, HSG failed to demonstrate these anomalies.

Conclusion : MR imaging satisfactorily demonstrated intrauterine lesions in nine of 11 patients with Asherman's syndrome, and was especially helpful in demonstrating associated uterine anomalies.

Index words : Uterus, abnormalities
Uterus, MR
Uterus, radiography

Asherman's syndrome is caused by intrauterine adhesions which result from scarring in the uterine cavity. Endometrial trauma or infection caused by postpartum or postabortion curettage are main causes of this syndrome (1), which is strongly suspected in women with postcurettage hypo- or amenorrhea, infertility, repeated pregnancy losses, and/or severe obstetrical complications, including postpartum hemorrhage and placental

retention (2-4). Radiographically, diagnosis has been most commonly supported by the findings of hysterosalpingography (HSG). When Asherman's syndrome develops in a uterus with congenital anomaly, correct diagnosis is very important. In such patients, the treatment for this syndrome may be different from the treatment appropriate for those without uterine anomalies. The treatment of such anomalies requires various surgical procedures, depending on individual subtype, but Asherman's syndrome can be treated by curettage and the insertion of an intrauterine device (IUD), or by a hysteroscopic procedure (5, 6)

For the characterization of individual uterine anomalies, HSG suffers from limitations, though MR imaging is excellent in this regard (7-9). Although MR imaging

¹Department of Diagnostic Radiology, Keimyung University, DongSan Medical Center

²Department of Obstetrics and Gynecology, Keimyung University, DongSan Medical Center

Received April 27, 1998 ; Accepted November 27, 1998

Address reprint requests to : Jung Sik Kim, M.D., Department of Diagnostic Radiology, Keimyung University, DongSan Medical Center, #194 DongSan Dong, Chung Ku, Taegu, 700-310, Korea.

Tel. 82-53-250-7766 Fax. 82-53-250-7766

findings in the uterus of patients with Asherman's syndromes have been described (10, 11), we found no previous report of the MR imaging findings in Asherman's syndrome associated with uterine anomalies. The purpose of this study was to assess the role of MR imaging in the detection of Asherman's syndrome, especially when this is associated with a congenital uterine anomaly.

Materials and Methods

MR imaging was performed in eleven patients in whom Asherman's syndrome was diagnosed on the basis of clinical and HSG findings. Eight of 11 patients were referred for evaluation of associated uterine anomalies, two for comparison of MR imaging with HSG in the detection of uterine synechiae less than 10 mm in diameter, and one, with cervical synechia, for evaluation of the endometrium, which could not be evaluated on HSG. All patients had a history of spontaneous abortion 1-5 times, and four had a history of induced abortion once or more. Nine patients had a history of hypomenorrhea.

HSG using a speculum, tenaculum and uterine elevator was performed under fluoroscopic control. A total of 10 to 15 ml of contrast medium (Telebrex 200, Taejun, Seoul, Korea) was injected into the uterine cavity slowly while monitoring uterine and tubal filling. Three anteroposterior images were obtained: a preliminary image prior to the introduction of contrast medium, and an early image after filling the uterine cavity but before tubal spillage, and a late image at the end of the examination.

MR imaging was performed on a 2.0-T imager

(Spectro 20000, Gold Star, Seoul, Korea) within one week of HSG. T1-weighted images with a repetition time of 600 msec and an echo time of 30 msec (TR/TE = 600/30), and T2-weighted images with TR/TE = 2000/60 were obtained. Section thickness was 8 mm with a 2 mm gap, matrix size was 256 x 320, and field of view was 24-30 cm. T1 and T2-weighted images were obtained in the sagittal planes. Finally, T2-weighted images with a small field of view (24 cm), and 5mm section thickness with a 2 mm gap, were obtained in the semicoronal plane parallel to the long axis of the uterine corpus.

Both HSG and MR images were retrospectively reviewed by two radiologists (J.S. Kim, H. Kim) without knowledge of the clinical findings. HSG images were interpreted first, and then MR images, and the results were recorded after both radiologists reached a consensus. HSG and MR images were compared with histopathologic findings in four patients who underwent laparotomy. In the remaining seven, who underwent dilatation and curettage (D & C) and insertion of an IUD, HSG was repeated after removal of the IUD, and the results were compared with previous HSG images.

During MR image analysis, the following parameters were recorded: 1. External fundal contour: convex, flat or concave; 2. Intercornual distance between the maximum lateral extents of the hyperintense endometrium; 3. Signal intensity characteristics of the uterus, endometrium and junctional zone; 4. Thickness and uniformity of the endometrium and junctional zone; 5. Signal intensity of the septum, which was divided into myometrial and fibrous tissue.

Classification of Asherman's syndrome based on

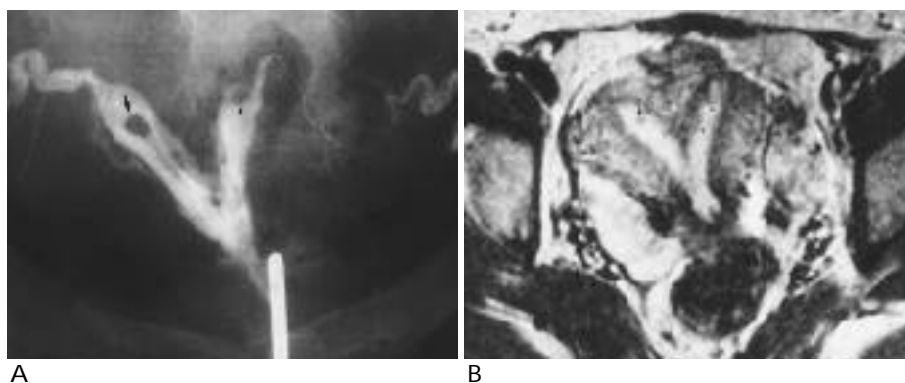


Fig. 1. Partial septate uterus with Asherman's syndrome (case 5)
A. HSG shows a partial duplicate uterine cavity with divergent angle of the endometrial cavity of 45° which is compatible with a partial septate uterus. A nodular filling defect in the right uterine horn (arrow) and a nodular luminal irregularity of the left uterine horn (arrowhead) are seen.
B. T2-weighted image shows an isointense myometrial septum and hypointense fibrous septum. The external

contour of the uterine fundus is flat. The intercornual distance is normal. A nodular hypointense focus in the right uterine horn (arrow) and focal irregular thickening of junctional zone (arrowheads) of the left uterine horn due to uterine synechia are well correlated with those seen on HSG.

HSG was in accordance with that of Toaff and Ballas: Grade I (a single small filling defect occupying up to one-tenth of the uterine area); Grade 2 (one or more filling defects occupying up to one-fifth of the uterine area); Grade 3 (filling defects occupying up to one-third of the uterine area); and Grade 4 (filling defects occupying most of the uterine area) (12).

Classification of uterine anomalies was in accordance with the modified classification of Buttram and Gibbons: class I (segmental Müllerian agenesis or hypoplasia); class II (unicornuate uterus); class III (uterine didelphys); class IV (bicornuate uterus); class V (septate uterus); and class VI (diethylstilbestrol related) (13). Classification of uterine anomalies based on HSG was in accordance with both Ott et al. (1) and Reuter et al. (14): class I (nonopacification of any segment of the Müllerian duct, and supported pelvic examination); class II (nonopacification of one of the paired Müllerian ducts); class III (two completely separate cervical canals opening into fusiform endometrial cavities, each ending in a solitary fallopian tube); class IV (two separate wide-angle uterine horns $> 105^\circ$); class V (two separate acute-angle uterine horns $< 75^\circ$); class VI (T-shaped uterine cavity).

Results

MR and HSG findings are summarized in Table 1. Asherman's syndrome without uterine anomaly was diagnosed in four patients, and Asherman's syndrome with uterine anomaly in seven. Associated uterine anomalies were complete septate uterus ($n = 1$), and partial septate uterus ($n = 6$). Four of seven patients with Asherman's syndrome associated with uterine anomaly underwent transabdominal metroplasty, while three of four without associated anomalies were treated with D & C and IUD insertion. One patient without uterine anomaly received no treatment because of detachment of uterine synechiae during HSG. The amount of menstrual flow increased in nine patients with hypomenorrhea following adequate treatment. Follow-up HSG after IUD removal in ten patients, two of whom also underwent MR imaging, revealed the complete disappearance of uterine filling defects in six patients and partial recovery in four.

In all patients, HSG demonstrated intrauterine filling defects which represented uterine synechia. MR imaging revealed findings of Asherman's syndrome in nine

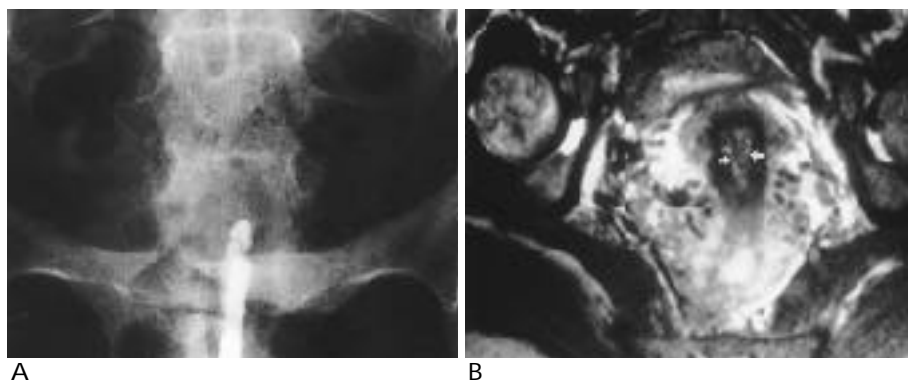


Fig. 2. Cervical synechia (case 10)
A. HSG shows complete obstruction of a cervical canal with luminal irregularities. Evaluation of the uterine cavity was impossible.
B. T2-weighted MR image shows a retroflected uterus with hypointense lesions of the cervical canal (arrows). However, the hyperintense uterine endometrial cavity is well preserved.

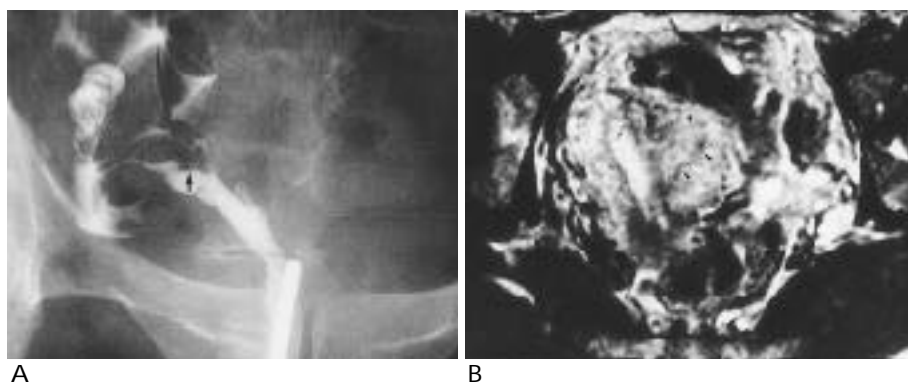


Fig. 3. Complete septate uterus with Asherman's syndrome (case 3)
A. HSG shows a single uterine horn with a single fallopian tube, which was misdiagnosed as a unicornuate uterus. Focal luminal irregularities in the uterine cavity (arrow) are noted.
B. T2-weighted image shows a complete septate uterus with a myometrial and fibrous septum. The external contour of the uterine fundus is flat. Low signal intensity of the endometrium of the left uterine horn (arrowheads) and a focal nodular thickening of junctional zone of the right uterine horn (arrow) by uterine synechia are noted.

a focal nodular thickening of junctional zone of the right uterine horn (arrow) by uterine synechia are noted.

of eleven patients, with findings of focal thickening of the junctional zone (n = 2), hypointense foci in the endometrium on both T1- and T2-weighted images (n = 1), or both these findings (n = 6) (Fig. 1). MR and HSG findings showed close correlation. In one patient (case 11), two small nodular filling defects were demonstrated in earlier HSG images, though in later images these had disappeared. MR imaging showed no abnormal

finding in this patient. In the other patient (case 7), in whom MR imaging did not demonstrate abnormal findings, HSG showed three small filling defects less than 5mm in diameter. However, in one patient with cervical synechia (case 10), in whom HSG failed to demonstrate changes in the uterine cavity due to obstruction of the cervical canal, MR imaging showed a well preserved endometrial cavity with involvement of synechia in the

Table 1. Summary of MR Imaging and HSG Findings of Asherman's Syndrome

Case /Age	Associated Uterine Anomaly / treatment	MR Imaging Findings	HSG Findings
1/28	(-) D & C and IUD insertion	two low signal foci in endometrium, BCD:30mm	two nodular filling defects
2/24	(-) D & C and IUD insertion	a wedge shaped thickening of junctional zone of intercornual area of uterine fundus, linear & nodular hypointense foci in endometrium, BCD: 25mm	awedge shaped filling defect with marginal irregularity, several nodular filling defects, angle : 90
3/37	Complete septate uterus D & C and IUD insertion Metroplasty	hypointense endometrium of left horn, focal thickening of junctional zone in right horn, flat fundus outwardly, proximal myometrial and distal fibrous septum. BCD: 45mm	single horn with filling defects
4/27	Partial septate uterus D & C and IUD insertion	a focal thickening of junctional zone, small fundal cleft (5mm).	a small filling defect in right cornus, angle : 120
5/29	Partial septate uterus D & C and IUD insertion Metroplasty	two focal thickening of junctional zone, a hypointense focus in endometrium.	two filling defects in both uterine cornus, angle : 45
6/26	Partial septate uterus D & C and IUD insertion Metroplasty	three focal thickening of endometrium, small fundal cleft (8mm), myometrial septum, BCD: 50mm	three filling defects in both uterine cornus, angle : 60
7/27	Partial septate uterus D & C and IUD insertion Metroplasty	flat fundus outwardly, myometrial septum, BCD: 50mm	three filling defects in both uterine cornus, angle : 70
8/30	Partial septate uterus D & C and IUD insertion	two focal thickening of junctional zone in left horn, a hypointense focus in endometrium, convex fundus outwardly, myometrial septum, CD: 46mm	three filling defects in left horn angle : 120
9/28	Partial septate uterus D & C and IUD insertion	a large hypointense focus in endometrium, a focal thickening of junctional zone, BCD: 30mm	a large filling defect in intercornual region
10/36	(-) D & C and IUD insertion	hypointense cervical canal, well preserved uterine cavity	obstruction of cervical canal without dye filling in uterine cavity,
11/24	(-) no treatment	normal BCD : 24mm	two nodular filling defects relieved in later image

D & C : dilatation and curratage, IUD : intrauterine device, BCD : bicornual distance, MR : magnetic resonance, HSG: hysterosalpingography

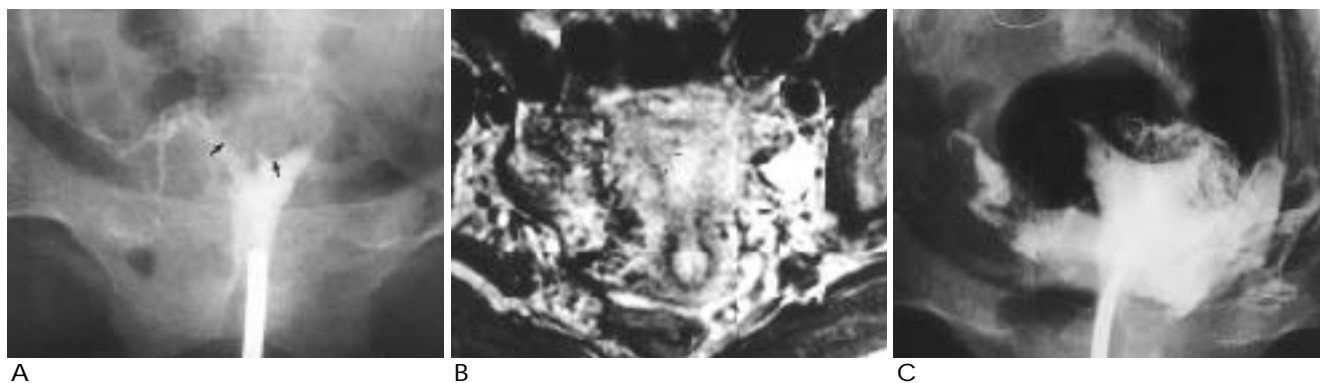


Fig. 4. Asherman's syndrome without uterine anomaly (case 2)

A. HSG shows a wedge shaped filling defect with luminal irregularities in a uterine fundus (arrows), which was misdiagnosed as a partial septate uterus with Asherman's syndrome

B. T2-weighted MR image shows no uterine anomaly but demonstrates a wedge-shaped hypointense lesion (arrows) in the intercornual region of the uterine fundus.

C. Follow-up HSG after D & C and IUD insertion shows disappearance of uterine synechia in the fundal region. Marked intravasation with opacification of the left pelvic venous system are noted.

cervical canal only (Fig. 2).

In seven patients with uterine anomalies, MR imaging permitted the correct diagnosis. The use of HSG, however, led to correct diagnosis in only three patients with partial septate uterus; in these three, the angle of divergence of the uterine cavities was less than 75. In one patient (case 3), who had a complete septate uterus with obliteration of the left uterine horn by synechia, MR images demonstrated both lesions correctly but HSG was incorrectly interpreted as a unicornuate uterus with Asherman's syndrome (Fig. 3). In another patient with Asherman's syndrome without uterine anomaly (case 2), MR images showed a wedge shape hypointense focus of uterine synechia in the endometrium of the uterine fundus, but the results of HSG were incorrectly interpreted as a septate uterus with Asherman's syndrome (Fig. 4). In two patients with partial septate uterus (case 4 and 8), MR images clearly showed myometrial septa, but because of the wide angle of the uterine horns, HSG was incorrectly interpreted as showing a bicornuate uterus.

Discussion

Asherman's syndrome and congenital uterine anomaly are two important causes of repeated termination of pregnancy. When both conditions exist in the same patient, correct diagnosis is difficult but important, since treatment of the two conditions differs.

In Asherman's syndrome, intrauterine adhesions obliterate part or all of the endometrial cavity and/or cervical canal. This sequela of uterine trauma is almost

always related to pregnancy, and usually to curettage performed to terminate a pregnancy or to evacuate an incomplete or missed abortion or the retained products of conception (15).

Uterine anomalies have a prevalence of up to 2-3 %, and approximately 25 % of women with uterine anomalies have fertility problems (13). Septate uterus is the most common anomaly and demonstrates the highest complication rate. It is associated with an 88 % abortion rate, attributed to poor vascularity of the septum. Where the uterus is bicornuate, the outcome is similar, with a 70 % abortion rate (5). Both septate and bicornuate uteri may be treated by transabdominal metroplasty, but for septate uterus, hysteroscopic metroplasty is now the treatment of choice (6). The differing treatment of septate and bicornuate uteri requires that the two are accurately differentiated, though in this respect HSG suffers from limitations in that it images only the internal architecture of the uterus and cannot evaluate the external uterine contour (11-15). According to Reuter et al. (14) the diagnostic accuracy of HSG in distinguishing septate uterus from bicornuate uterus was 55 %, though when ultrasonography and HSG were used together, diagnostic accuracy improved to 90 %, with all errors noncritical. The result of HSG using the angle criteria recommended by Reuter et al. (15) for the diagnosis of septate uterus was accurate in only three of our seven patients. One patient with complete septate uterus (case 3) was misdiagnosed as unicornuate uterus by HSG because of complete obliteration of the left uterine horn by synechia.

MR imaging has proved to be excellent for the delin-

eation of septa, the signal intensity characteristics of which enable differentiation between myometrial and fibrous septum (8, 9). Carrington et al. (8) and Pellento et al. (9) reported that MR imaging permitted correct diagnosis of uterine anomalies in all their patients, and this was also true in our study.

For correct interpretation, MR images obtained in a plane parallel to the long axis of the uterus were essential. This allowed evaluation of the external uterine contour, which was important in distinguishing septate from bicornuate uterus. In addition, it permitted evaluation of the whole area of the uterine cavity and junctional zone. The T2-weighted image of the uterine cavity in this plane was comparable with the HSG image, and in nine of 11 patients clearly demonstrated the lesions of Asherman's syndrome.

MR imaging findings in three cases of Asherman's syndrome were reported by Woodward et al. (11) and Dykes et al. (10). T2-weighted images showed that a hypointense band traversed the endometrium, and that normal endometrium and junctional zone signals were completely absent. All their previously reported cases involved severe synechiae and did not correlate with HSG findings. However, our study included less severe cases of Asherman's syndrome and patients with associated uterine anomalies. Our study demonstrated various MR findings of Asherman's syndrome, according to the severity of the disease, and the presence or absence of associated uterine anomalies. MR findings of Asherman's syndrome included focal thickening of the uterine junctional zone, hypointense foci in the endometrium, or both. To determine the significance of individual findings, further study with a larger number of cases will be necessary.

The limitations of this study were that uterine anomaly was histologically confirmed in only four of seven patients with both uterine anomaly and Asherman's syndrome, and that Asherman's syndrome in the remaining four patients without uterine anomaly was diagnosed by clinical, HSG and MR findings, without hysteroscopic confirmation.

In conclusion, MR imaging clearly demonstrated uter-

ine lesions in patients with Asherman's syndrome, and was comparable with the findings of HSG. MR imaging also provided further important information regarding associated uterine anomalies.

References

1. Ott DJ, Faye JA. *Uterine body abnormalities*. In Ott DJ, Faye JA. *Hysterosalpingography: A Text and Atlas*. Baltimore-Murich Urban & Schwarzenberg. 1991:85-101
2. Jewelewicz R, Khalaf S, Neuwirth RS. Obstetric complications after treatment of intrauterine synechiae (Asherman's syndrome). *Obstet Gynecol* 1976;47:701-705
3. Fridman A, Detazio J, Decherney A. Severe obstetric complications after aggressive treatment of Asherman's syndrome. *Obstet Gynecol* 1986;67:864-867
4. Shaffer W. Role of uterine adhesions in the cause of multiple pregnancy losses. *Clin Obstet gynecol* 1986;29:912-924
5. Cunningham FG, McDonald PC, Leveno KJ, Gant NF, Gilstrap LC. *Developmental abnormalities of the reproductive tract*. In Cunningham FG, McDonald PC, Leveno KJ, Gant NF, Gilstrap LC, Hankins GDV, Clark SL. *Williams obstetrics*. 19th ed. East Narwalk, Conn. Appleton & Lange. 1992:721-732
6. Brooks PG. Hysteroscopic surgery using the resectoscope: myomas, abrasions, septate and synechiae: Does preoperative medication help? *Clin Obstet Gynecol* 1992;35:249-255
7. Fedele L, Dorta M, Brioschi D, Massari C, Canadian GB. Magnetic resonance evaluation of double uteri. *Obstet Gynecol* 1989;74:844-847
8. Carrington BM, Hricak H, Nuruddin RN, Secaf E, Laros RK, Hill EC. Mullerian duct anomalies: MR imaging evaluation. *Radiology* 1990;176:715-720
9. Pellerito JS, McCarthy SM, Doyle MB, Glickman MG, Dechemey AH. Diagnosis of uterine anomalies: relative accuracy of MR imaging, endovaginal sonography, and hysterosalpingography. *Radiology* 1992;183:795-800
10. Dylces TA, Isler RJ, Mclean AC. MR imaging of Asherman's syndrome: total endometrial obliteration. *J Comput Assist Tomogr* 1991;5:858-860
11. Woodward PS, Wagner BJ, Farley TE. MR imaging in the evaluation of female infertility. *Radiographics* 1993;13:293-310
12. Foaff R and Ballas S. Traumatic hypomenorrhea amenorrhea (Asherman's syndrome). *Fertil Steril* 1978;30:379-388
13. Buttam VC, Gibbons WE. Mullerian anomalies: a proposed classification: an analysis of 144 cases. *Fertil Steril* 1979;32:40-46
14. Reuter KL, Daly DC, Cohen SM. Septate versus bicornuate uteri: errors in imaging diagnosis. *Radiology* 1989;172:747-752
15. Ler-Toaff AS, Toaff MF. *Diagnostic imaging in female infertility*. In Friedman AC Radecki PD, Ler-Toaff AS, Hilpert PL. *Clinical pelvic imaging*. 1st ed. St. Louis, The C.V. Mosby. 1990: 38-442

